74.57, H 5.93, N 6.87; found: C 73.58, H 5.69, N 7.06. These results indicate the loss of 0.5 *o*-xylene per metal: calculated values for $[Ni(\mathbf{2})_2(NO_3)_2 \cdot 3.5(o\text{-xylene})]$: C 73.85, H 5.77, N 7.18.

Crystal data for **4**: The crystals were prepared in the same way as above but benzene was used instead of *o*-xylene. However few crystals were obtained with some powdery material (in 15% yield). Monoclinic, $P2_1/n$, $a = 13.570(2)$, $b = 19.874(3)$, $c = 49.646(7)$ Å, $\beta = 96.815(3)^\circ$, $V = 13294(3)$ Å^3, $Z = 8$, $\rho_{calcd} = 1.237$ g cm^{-3}, 23360 unique reflections out of 68329 with $I > 2\sigma(I)$, $1.32 < \theta < 25^\circ$, final R factors $R_1 = 0.1561$; $wR_2 = 0.3795$. The data for both **3** and **4** were measured on a Siemens SMART/CCD diffractometer ($Mo_{K\alpha}$ radiation $\lambda = 0.71073$ Å) at 193 K. An empirical absorption correction was applied by using the SADABS program. Non-hydrogen atoms were refined anisotropically and hydrogen atoms were fixed at calculated positions and refined using a riding model. Crystallographic data (excluding structure factors) for the structures reported in this paper have been deposited with the Cambridge Crystallographic Data Centre as supplementary publication nos. CCDC-141218 (**3**), and CCDC-141217 (**4**). Copies of the data can be obtained free of charge on application to CCDC, 12 Union Road, Cambridge CB21EZ, UK (fax: (+44) 1223-336-033; e-mail: deposit@ccdc.cam.ac.uk).

Received: March 6, 2000
Revised: August 14, 2000 [Z14813]

[1] Only eight polymeric structures were published before 1990 for reactions of **1** with transition metals, while from 1990 to 1998 about 70 polymeric structures were published. Statistics were taken from Cambridge Structural Database: Version 5.17 (197481 Structures, April, 1999 release): F. H. Allen, O. Kennard, *Chemical Des. Autom. News* **1993**, *8*, 31.

[2] Recent references on coordination polymers with **1** and transition metals: a) K. Biradha, C. Seward, M. J. Zaworotko, *Angew. Chem.* **1999**, *111*, 584; *Angew. Chem. Int. Ed.* **1999**, *38*, 492; b) K. Biradha, K. V. Domasevitch, B. Moulton, C. Seward, M. J. Zaworotko, *Chem. Commun.* **1999**, 1327; c) H. Gudbjartson, K. Biradha, K. M. Poirier, M. J. Zaworotko, *J. Am. Chem. Soc.* **1999**, *121*, 2599; d) O. Wang, X. Wu, W. Zhang, T. Sheng, P. Lin, J. Li, *Inorg. Chem.* **1999**, *38*, 2223; e) M.-L. Tong, B.-H. Ye, J.-W. Cai, X.-M. Chen, S. W. Ng, *Inorg. Chem.* **1998**, *37*, 2645; f) L. R. MacGillivray, R. H. Groeneman, J. L. Atwood, *J. Am. Chem. Soc.* **1998**, *120*, 2676; g) C.-Y. Su, B.-S. Kang, H.-Q. Liu, Q.-G. Wang, T. C. W. Mak, *Chem. Commun.* **1998**, 1551; h) D. Hagrman, R. P. Hammond, R. Haushalter, J. Zubieta, *Chem. Mater.* **1998**, *10*, 2091; i) J. Lu, C. Yu, T. Niu, T. Paliwala, G. Crisci, F. Somosa, A. J. Jacobson, *Inorg. Chem.* **1998**, *37*, 4637; j) M. Kondo, T. Yoshitomi, K. Seki, H. Matsuzaka, S. Kitagawa, *Angew. Chem.* **1997**, *109*, 1844; *Angew. Chem. Int. Ed. Engl.* **1997**, *36*, 1725; k) O. M. Yaghi, H. Li, T. L. Groy, *Inorg. Chem.* **1997**, *36*, 4292.

[3] R. W. Gable, B. F. Hoskins, R. Robson, *J. Chem. Soc. Chem. Commun.* **1990**, 1677.

[4] M. Fujita, Y. J. Kwon, S. Washizu, K. Ogura, *J. Am. Chem. Soc.* **1994**, *116*, 1151.

[5] a) M. Fujita, Y.-J. Kwon, M. Miyazawa, K. Ogura, *Chem. Commun.* **1994**, 1977; b) J. A. Real, E. Andrés, M. C. Muñoz, M. Julve, T. Granier, A. Bousseksou, F. Varret, *Science* **1995**, *268*, 265; c) T. L. Hennigar, D. C. MacQuarrie, P. Losier, R. D. Rogers, M. J. Zaworotko, *Angew. Chem.* **1997**, *109*, 1044; *Angew. Chem. Int. Ed. Engl.* **1997**, *36*, 972; d) Y.-B. Dong, R. C. Layland, M. D. Smith, N. G. Pschirer, U. H. F. Bunz, H.-C. zur Loye, *Inorg. Chem.* **1999**, *38*, 3056.

[6] a) Quite recently a three-dimensional coordination polymer was characterized following removal of guest molecule by single-crystal X-ray diffraction: H. Li, M. Eddaoudi, M. O'Keeffe, O. M. Yaghi, *Nature* **1999**, *402*, 276; b) for zeolite analogues see: D. W. Breck in *Zeolite Molecular Sieves*, Wiley, New York, **1974**.

[7] Crystal data for **3** after removal of guest molecule: monoclinic, $C2/c$, $a = 26.234(5)$, $b = 19.839(3)$, $c = 13.236(2)$ Å, $\beta = 109.514(4)^\circ$, $V = 6493(2)$ Å^3, $Z = 4$, $\rho_{calcd} = 0.818$ g cm^{-3}, 2541 unique reflections out of 7718 with $I > 2\sigma(I)$, final R factors $R_1 = 0.1943$, $wR_2 = 0.4494$, largest difference peak and hole 2.126 and -0.764 e Å^{-3}. Elemental analysis suggests that the crystal absorbed water from atmosphere: calcd for $[Ni(\mathbf{2})_2(NO_3)_2] \cdot 1.5(H_2O)$: C 63.94, H 4.27, N 10.17; found: C 64.17, H 3.90, N 9.96.

[8] The data collection for **4** at room temperature resulted in different cell constants and space group as well as disordered ligands and nitrates. All the benzene molecules were located with relatively high thermal motions in comparison to those found for the low-temperature structure, but the MeOH molecules could not be located at this temperature. Monoclinic, Cm, $a = 12.731(7)$, $b = 19.912(9)$, $c = 13.902(7)$ Å, $\beta = 96.544(1)^\circ$, $V = 3501(3)$ Å^3, $Z = 2$, $\rho_{calcd} = 1.129$ g cm^{-3}, 3846 unique reflections out of 5211 with $I > 2\sigma(I)$, final R factors $R_1 = 0.0887$; $wR_2 = 0.2166$.

[9] One of the MeOH molecules which is close to the corner of a square interacts with benzene through a C–H···O hydrogen bond (H···O, 2.522 Å; C···O 3.441 Å; C–H···O 169.8°). The square **B** (diagonal – diagonal distances: 26.067 and 30.099 Å) is more distorted than square **A** (diagonal – diagonal distances: 27.911 and 28.270 Å).

The Electrical Properties of Gold Nanoparticle Assemblies Linked by DNA**

So-Jung Park, Anne A. Lazarides, Chad A. Mirkin,* Paul W. Brazis, Carl R. Kannewurf,* and Robert L. Letsinger

Electron transport through DNA has been one of the most intensely debated subjects in chemistry over the past five years.[1] Some scientists claim that DNA is able to transport electrons efficiently, while others believe it to be an insulator. In a seemingly disparate field of study, a great deal of effort has been devoted to examining the electrical properties of nanoparticle-based materials.[2–5] Indeed, many research groups have explored ways to assemble nanoparticles into two- and three-dimensional networks and have investigated the electronic properties of such structures. However, virtually nothing is known about the electrical properties of nanoparticle-based materials linked with DNA.

[*] Prof. C. A. Mirkin, S.-J. Park, Dr. A. A. Lazarides
Department of Chemistry and Center for Nanofabrication and Molecular Self Assembly
Northwestern University
2145 Sheridan Road, Evanston, IL 60208-3113 (USA)
Fax: (+1) 847-467-5123
E-mail: camirkin@chem.nwu.edu
Prof. C. R. Kannewurf, P. W. Brazis
Department of Electrical and Computer Engineering
Northwestern University
2145 Sheridan Road, Evanston, IL 60208-3118 (USA)
Fax: (+1) 847-491-4455
E-mail: c.kannewurf@ece.nwu.edu
Prof. R. L. Letsinger
Department of Chemistry, Northwestern University
2145 Sheridan Road, Evanston, IL 60208-3113 (USA)

[**] C.A.M. acknowledges the NSF, the ARO, and NIH for support of this research. R.L.L. acknowledges the NIH. C.R.K. and C.A.M. acknowledge support by the NSF through the Northwestern University MRC (Grant DMR 96-32472). The DND-CAT Synchrotron Research Center is supported by E.I. Dupont de Nemours & Co., The Dow Chemical Company, the U.S. National Science Foundation (Grant DMR-9304725), and the State of Illinois through the Department of Commerce and the Board of Higher Education (Grant IBHE HECA NWU 96). Use of the Advanced Photon Source was supported by the U.S. Department of Energy, Basic Energy Sciences, Office of Energy Research (Contract No. W-31-102-Eng-38).

  1433-7851/00/3921-3845 $ 17.50+.50/0

In 1996 we reported a new approach to materials synthesis which utilized inorganic nanoparticles as building blocks and chemically modified synthetic duplex DNA as the molecules interconnecting the particles.[6] Since that report, a great deal of effort has been devoted to studying the optical properties of such structures. Importantly, an understanding of those optical properties has led to the development of a series of highly sensitive and selective colorimetric detection methods for DNA.[7] Moreover, this programmed assembly methodology, by virtue of the oligonucleotide sequence, has provided an excellent opportunity to tailor the architectural parameters of nanoparticle-based structures assembled with DNA.[8] Such parameters include nanoparticle size and composition, particle periodicity, and interparticle distance. One of the intriguing outstanding issues in this new field pertains to the use of such materials in electronic applications. At the heart of this issue is the following question: can nanoparticles assembled by DNA still conduct electricity or will the DNA interconnects, which are heavily loaded on each particle,[9] act as insulating shells? Herein, we examine the electrical conductivities of these materials as a function of temperature, oligonucleotide length, and relative humidity. The DNA-linked nanoparticle structures have been characterized by field-emission scanning electron microscopy (FE-SEM), synchrotron small angle X-ray scattering (SAXS) experiments, thermal denaturation profiles, and UV/Vis spectroscopy.

In a typical experiment citrate-stabilized 13-nm gold nanoparticles were modified with 3′ and 5′ alkanethiol-capped 12-mer oligonucleotides (**1** and **2**, respectively). DNA strands with lengths of 24, 48, and 72 bases (**3**–**5**) were used as linkers (Scheme 1). Nanoparticle assemblies were constructed by adding **1**-modified gold nanoparticles (652 μL, 9.7 nM) and **2**-modified gold nanoparticles (652 μL, 9.7 nM) to linker DNA **3**, **4**, or **5** (30 μL, 10 μM). After full precipitation, the aggregates were washed with 0.3 M CH_3COONH_4 solution to remove excess linker DNA and NaCl. Lyophilization (10^{-3}–10^{-2} torr) of the aggregate to dryness resulted in pellets and removal of the volatile salt, CH_3COONH_4. Unfunctionalized, citrate-stabilized particles, prepared by the Frens method,[10] were dried as a film and used for comparison purposes.

The resulting dried aggregates had a color resembling tarnished brass and were very brittle. FE-SEM images demonstrate that oligonucleotide-modified nanoparticles remain intact upon drying (Figure 1 a) while citrate-stabilized nanoparticles fuse to one another (Figure 1 b). Significantly, the dried DNA-linked aggregates could be redispersed in 0.3 M PBS buffer (1 mL) and exhibit excellent melting properties; heating such a dispersion to 60 °C results in dehybridization of the DNA interconnects to yield a red solution of dispersed nanoparticles (Figure 2). This observation com-

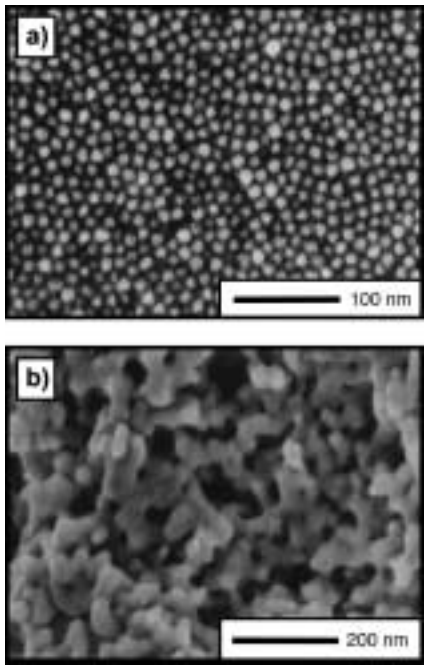

Figure 1. Scanning electron microscopy images of: a) DNA-modified gold nanoparticles, and b) citrate-stabilized gold nanoparticles dried on indium tin oxide.

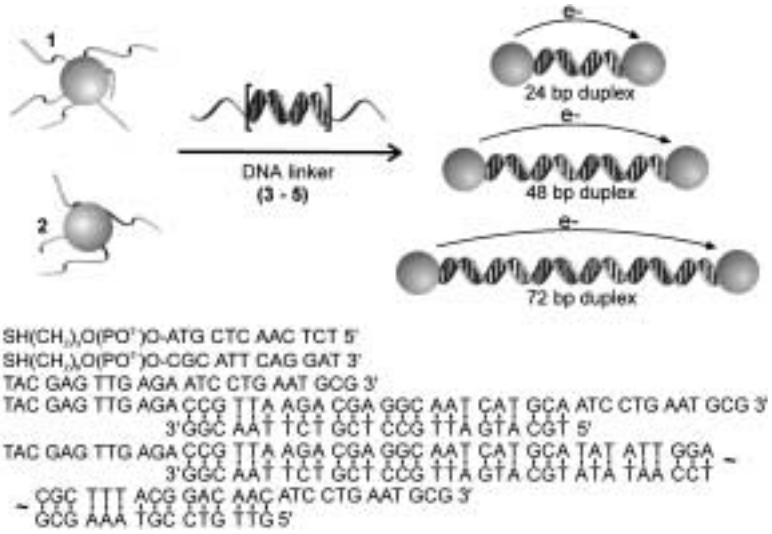

Scheme 1. Schematic representation showing Au nanoparticle assembly with different length DNA linkers.

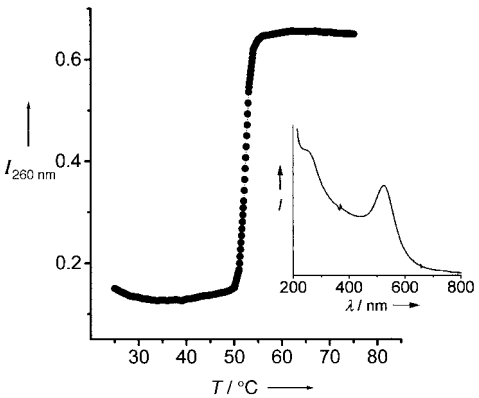

Figure 2. Thermal dissociation curve for dried aggregates linked by **3** and redispersed in 0.3 M PBS buffer. The extinction at 260 nm was obtained at 1° intervals as the temperature was increased from 25 to 75 °C with a holding time of 1 min per degree. Inset: UV/Vis spectrum of the redispersed dried aggregates measured at 62 °C.

  1433-7851/00/3921-3846 $ 17.50+.50/0 *Angew. Chem. Int. Ed.* **2000**, *39*, No. 21

bined with the FE-SEM data conclusively demonstrates that DNA-modified gold nanoparticles are not irreversibly aggregated upon drying.

The electrical conductivities of the three samples (dried aggregates linked by **3**, **4**, and **5**) were measured by the four-probe method. Surprisingly, the conductivities of the aggregates formed from all three linkers ranged from 10^{-5} to $10^{-4}\,S\,cm^{-1}$ at room temperature, and they showed similar temperature-dependent behavior (Figure 3). The conductivities of the DNA-linked aggregates showed Arrhenius behavior up to about 190 K, which is characteristic of a nonmetallic

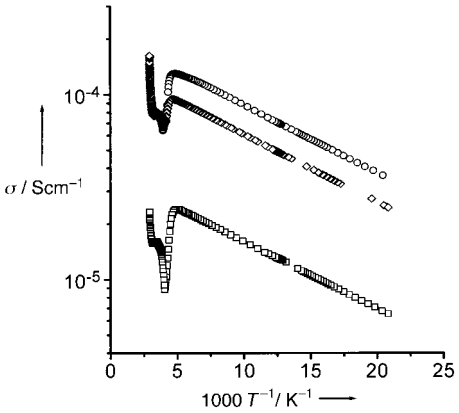

Figure 3. Plot of the conductivity as a function of temperature for gold nanoparticle assemblies linked by 24-, 48-, and 72-mer DNA (**3**–**5**). ○ = 24-mer-linked; ◇ = 48-mer-linked; □ = 72-mer-linked assemblies.

material. Activation energies of charge transport (E_a) can be obtained from a plot of lnσ versus $1/T$ using Equation (1), where σ is the electrical conductivity, σ_o is a constant, k is the Boltzmann constant, and T is the temperature.

$$\sigma = \sigma_o \exp[-E_a/(kT)] \quad (1)$$

The average activation energies calculated from three measurements are 7.4 ± 0.2 meV, 7.5 ± 0.3 meV, and 7.6 ± 0.4 meV for the 24-, 48-, and 72-mer-linked aggregates, respectively. Conductivity data obtained between 50 and 150 K were used for these calculations.

Since the electrical properties of these types of materials should depend on the distance between the particles, synchrotron SAXS experiments were used to determine interparticle distances of the dispersed and dried aggregates. Scattered intensities (I) as a function of $s = 2\sin(\theta)/\lambda$, where 2θ is the scattering angle and λ is the wavelength of the incident radiation, are presented in Figure 4. The s values of the first peaks indicate characteristic distances of $d = 1/s$. The position of the first peaks drastically changes from s values of $0.063\,nm^{-1}$, $0.048\,nm^{-1}$, and $0.037\,nm^{-1}$ for the 24-, 48-, and 72-mer-linked aggregates, respectively, to an s value of $0.087\,nm^{-1}$ for all three aggregate structures upon drying. This result indicates that upon drying the aggregates, the interparticle distances decrease significantly to the point where the particles are almost touching. In other words, dried aggregates have interparticle distances that are virtually

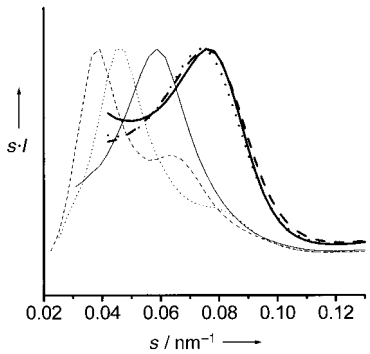

Figure 4. SAXS of gold nanoparticle aggregates linked by **3**–**5**. Thin lines: SAXS of aggregates in 0.3 M PBS buffer. The first peak of the DNA-linked aggregates shifts to smaller values of s as the length of the oligonucleotide linker is increased. Thick lines: SAXS of dried aggregates. The first peaks shift to larger values of s upon drying and are not dependent on the length of the DNA linker. ——: 24-mer-linked; ●●●●: 48-mer-linked; - - - -: 72-mer-linked aggregates.

independent of the length of the linker, while wet aggregates exhibit interparticle distances that are directly dependent on the length of the linker. This finding explains why similar activation energies are observed for the three different linker systems in the conductivity experiments involving dried pellets. Moreover, it also explains why relatively high conductivities are observed, regardless of how one views the electronic properties of DNA. Indeed, these results suggest that conductivity in these systems is a result of capacitive charging, much like aggregates formed from particles with short alkanethiol ligands.[2, 3] Finally, unlike the DNA-linked materials, the dried film of citrate-stabilized gold nanoparticles showed metallic behavior. This is consistent with the SEM data, which show that particles within such films fuse together (Figure 1b).

Above 190 K the conductivities of the DNA-linked samples showed an anomalous dipping behavior. For all the samples the conductivity starts to decrease abruptly at approximately 190 K and continues to decrease until approximately 250 K, at which point it increases again (Figure 3). To investigate this unusual behavior in detail the electrical conductivity was measured as the sample was cooled and warmed repeatedly (Figure 5). Interestingly, the dip in conductivity only occurred in the direction of increasing temperature. Since DNA is hydrophilic and water could potentially affect the electrical properties of the hybrid structures, the effect of relative humidity on the conductivity of the gold aggregates was examined. The resistance increased by a factor of ten when the humidity was increased from 1 to 100%. It should be noted that the characteristic dip was very weak when the sample was kept in a vacuum (10^{-6} Torr) for 48 h prior to the conductivity measurement. From these observations we conclude that the unusual dip and then rise in conductivity above 190 K is associated with water melting and the hygroscopic nature of the DNA, which temporarily increases the interparticle distance (until evaporation takes place). SAXS measurements on a dried aggregate that was wetted with 0.3 M PBS buffer showed an approximately twofold increase in interparticle distance, which is consistent with the above hypothesis.

  1433-7851/00/3921-3847 $ 17.50+.50/0

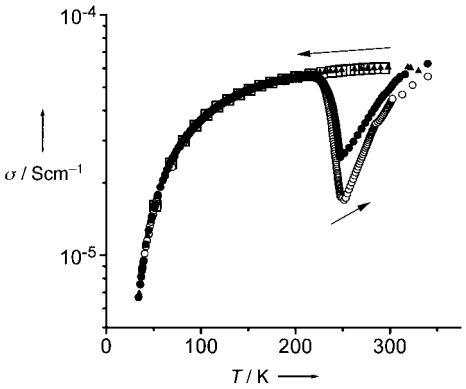

Figure 5. Electrical conductivity of gold nanoparticle assemblies linked by **3** as a function of temperature cycling. The first data collection was cycled between 294 and 4.2 K, and the second data collection was cycled between 340 and 4.2 K. The arrows indicate the direction of the temperature change. □ = first cooling; ○ = first warming; ▲ = second cooling; ● = second warming.

These studies are important for the following reasons. First, they show that one can use the molecular recognition properties of DNA to assemble nanoparticle-based materials without passivating them or destroying their discrete structural or electrical properties. If these DNA-functionalized particles are to be used to study electrical transport in three-dimensional macroscopic assemblies or even lithographically patterned structures,[11] it is imperative that their electrical transport properties be delineated. Second, it shows that the conductivities of the dried assemblies formed with linkers of 24 to 72 base pairs are virtually independent of the length of the linker. This observation is likely a result of the removal of water and the use of a volatile salt in these experiments; indeed, the free volume created by the removal of solvent and salt allows the DNA to be compressed on the surface and the close approach of the particles within the aggregates. Third, the aggregates with the DNA-protected nanoparticles behave as semiconductors, while films formed from citrate-stabilized particles exhibit irreversible particle fusion and metallic behavior. Finally, these results point toward the intriguing possibility of using these materials in DNA diagnostic applications where sequence-specific binding events between nanoparticles functionalized with oligonucleotides and target DNA effect the closing of a circuit and a dramatic increase in conductivity (that is, from an insulator to a semiconductor).

Experimental Section

Preparation of DNA-modified gold nanoparticles and linker DNA strands: Synthesis of alkanethiol-capped oligonucleotides (**1** and **2**) and immobilization of them on gold nanoparticles are described elsewhere.[7b] Linker DNA strands (**3**–**5**) were synthesized and purified by literature methods.[7b, 8c] The DNA-modified nanoparticles and DNA linkers were stored in 0.3 M NaCl, 10 mM phosphate (pH 7) buffer (referred to as 0.3 M PBS) prior to use.

Conductivity measurements: The electrical conductivity was measured by the four-probe technique.[12] Electrical contacts consisted of fine gold wires (25 and 60 μm diameter) attached to pellets with gold paste (Ted Pella). The sample dimensions were $0.185 \times 0.370 \times 0.056$ mm, $0.352 \times 0.722 \times 0.017$ mm, and $0.278 \times 0.463 \times 0.035$ mm for the 24-mer-linked, 48-mer-linked, and 72-mer-linked aggregates, respectively. Samples were cooled in a moderate vacuum (10^{-3} to 10^{-2} torr), and conductivity was measured as the temperature was increased under a dry, low pressure of helium gas unless otherwise specified. The sample chamber was insulated from light in order to eliminate possible optoelectronic effects. Excitation currents were kept at or below 100 nA, and the voltage across the entire sample was limited to a maximum of 20 V.

SAXS measurements: The SAXS experiments[13] were performed at the Dupont-Northwestern-Dow Collaborative Access Team (DND-CAT) Sector 5 of the Advanced Photon Source, Argonne National Laboratory with X-rays of wavelength 1.54 Å. Aqueous samples were placed in 0.8-mm flat cells between Kapton windows. Dried samples were adhered to Kapton tape and supported by flat cells. Two sets of slits were used to define and collimate the X-ray beam and a pinhole was used to remove parasitic scattering. Samples were irradiated with a 0.3×0.3 mm beam and scattered radiation was detected with a CCD area detector. The 2D-scattering data were azimuthally averaged, and the radial coordinate of the resulting 1D profiles of scattered intensity was transformed into a scattering angle. All data were corrected for background scattering and sample absorption. Buffer scattering was subtracted from the solution samples.

Received: July 10, 2000 [Z 15427]

[1] a) S. O. Kelley, J. K. Barton, *Science* **1999**, *283*, 375–381; b) N. J. Turro, J. K. Barton, *J. Biol. Inorg. Chem.* **1998**, *3*, 201–209; c) F. D. Lewis, R. L. Letsinger, *J. Biol. Inorg. Chem.* **1998**, *3*, 215–221; d) M. Ratner, *Nature* **1999**, *397*, 480–481; e) Y. Okahata, T. Kabayashi, K. Tanaka, M. Shimomura, *J. Am. Chem. Soc.* **1998**, *120*, 6165–6166.

[2] R. H. Terrill, T. A. Postlethwaite, C.-H. Chen, C.-D. Poon, A. Terzis, A. Chen, J. E. Hutchison, M. R. Clark, G. Wignall, J. D. Londono, R. Superfine, M. Falvo, C. S. Johnson, Jr., E. T. Samulski, R. W. Murray, *J. Am. Chem. Soc.* **1995**, *117*, 12537–12548.

[3] a) M. Brust, D. Bethell, D. J. Schiffrin, C. Kiely, *Adv. Mater.* **1996**, *7*, 795–797; b) D. Bethell, M. Brust, D. J. Schiffrin, C. Kiely, *J. Electroanal. Chem.* **1996**, *409*, 137–143; c) M. Brust, D. Bethell, C. Kiely, D. J. Schiffrin, *Langmuir* **1998**, *14*, 5425–5429.

[4] M. D. Musick, C. D. Keating, M. H. Keefe, M. J. Natan, *Chem. Mater.* **1997**, *9*, 1499–1501.

[5] C. P. Collier, R. J. Saykally, J. J. Shiang, S. E. Henrichs, J. R. Heath, *Science* **1997**, *277*, 1978–1981.

[6] C. A. Mirkin, R. L. Letsinger, R. C. Mucic, J. J. Storhoff, *Nature* **1996**, *382*, 607–609.

[7] a) R. Elghanian, J. J. Storhoff, R. C. Mucic, R. L. Letsinger, C. A. Mirkin, *Science* **1997**, *277*, 1078–1081; b) J. J. Storhoff, R. Elghanian, R. C. Mucic, C. A. Mirkin, R. L. Letsinger, *J. Am. Chem. Soc.* **1998**, *120*, 1959–1964; c) T. A. Taton, C. A. Mirkin, R. L. Letsinger, *Science* **2000**, *289*, 1757–1760.

[8] a) R. C. Mucic, J. J. Storhoff, C. A. Mirkin, R. L. Letsinger, *J. Am. Chem. Soc.* **1998**, *120*, 12674–12675; b) G. P. Mitchell, C. A. Mirkin, R. L. Letsinger, *J. Am. Chem. Soc.* **1999**, *121*, 8122–8123; c) J. J. Storhoff, A. A. Lazarides, C. A. Mirkin, R. L. Letsinger, R. C. Mucic, G. C. Schatz, *J. Am. Chem. Soc.* **2000**, *122*, 4640–4650.

[9] R. C. Mucic, PhD thesis, Northwestern University, IL, USA, **1999**.

[10] G. Frens, *Nat. Phys. Sci.* **1973**, *241*, 20–22.

[11] R. D. Piner, J. Zhu, F. Xu, S. Hong, C. A. Mirkin, *Science* **1999**, *283*, 661–663; S. Hong, J. Zhu, C. A. Mirkin, *Science* **1999**, *286*, 523–525; S. Hong, C. A. Mirkin, *Science* **2000**, *288*, 1808–1811.

[12] J. W. Lyding, H. O. Morey, T. J. Marks, C. R. K. Kannerwurf, *IEEE Trans. Instrum. Meas.* **1998**, *37*, 76–80.

[13] A. Guinier, G. Fournet, *Small angle scattering of X-rays*, Wiley, New York, **1955**.

  1433-7851/00/3921-3848 $ 17.50+.50/0